SUPPLEMENTAL METHODS

Immunohistochemistry.

Assistance in sample processing was provided by the University of North Carolina Center for Gastrointestinal Biology and Disease. Tumors, lymph nodes, spleens, and lungs were fixed in 10% formalin, embedded in paraffin, sectioned, deparaffinized (Histoclear, National Diagnostics), and stained using H&E for histological analysis. Slides were counterstained with hematoxylin and then mounted with Cytoseal XYL (Richard-Allan Scientific). The Translational Pathology Laboratory (TPL) at University of North Carolina Chapel Hill scanned in the slides at 20X objective, which were then analyzed using Spectrum software (Aperio Technologies, Vista, CA). CD31 antibody was purchased from Abcam (AB28364), used at a dilution of 1:50 and staining was performed by the TPL.

Quantification of melanin within lymph node metastasis.

Lymph nodes were stained with H&E by the UNC Center for GI Biology and Disease (CGDB). Slides were scanned in by TPL and analyzed using Spectrum software as above. 15-20 representative pictures were taken at 20X objective from lymph nodes from multiple mice of each cohort: *Pten*; *Braf*, *Pten*; *Braf*; *Hif1*$^{L/L}$, and *Pten*; *Braf; Hif2*$^{L/L}$. A blinded reviewer (B.K.) then quantified the percentage of melanin within the subcapsular sinus of each lymph node.

Chromatin Immuoprecipitation and Real Time PCR.

Chromatin for ChIP was prepared from A375 SM melanoma cells incubated under either normoxic (21% O_2) or hypoxic (1% O_2) conditions by fixing the cells in 1% formaldehyde for 10 minutes followed by quenching with 125mM glycine for 5 minutes. Cells were sonicated and then pelleted to isolate the chromatin. ChIP was performed using anti-HIF1α (Novus Biologicals NS100-134), anti-HIF2α (Novus Biologicals NB100-122) and anti-IGG antibody (Cell Signaling 2729S). Briefly, 4μg of the appropriate antibody was incubated with Protein A/G UltraLink Resin (Thermo Scientific) and allowed to bind for each ChIP reaction. Equivalent amounts of chromatin were added to the antibody-linked beads and incubated overnight at 4C. Supernatant was then collected and reverse cross-linked for analysis by RT-PCR. DNA were analyzed in duplicate using QuantiTect SYBR Green RT-PCR Kit (Qiagen). Relative concentrations were determined by $2^{-(Ct-Ct)}$, where Ct is the mean threshold after normalizing to input levels. Primers used for PCR were designed from HRE elements located in the promoter regions of PDGFRα and FAK (Supplementary Table 4). Positive and negative controls for both HIF1α and HIF2α were used (ENGL3 for HIF1α, AARCD3 HIF2α, and an upstream region of the VEGF promoter for the negative control).

Wound closure assay

A375 SM and WM2664 cells were plated and allowed to reach near confluence. A scratch was generated in a uniform manner and the cells were placed in

normoxia or hypoxia for 16 hours. Representative photomicrographs of the wound closure were taken using an Olympus IX51 microscope. Quantification of wound closure was performed using ImageJ software.

Extracellular Passive Microrheology.

Passive measurements used microbeads (2 μm diameter, Invitrogen) coated with fibronectin to form attachment to integrin receptors on the surface of the cells. Brownian motion of the beads was tracked using Video Spot Tracker (CISMM.org) and the mean squared displacement (MSD) of the trajectories was computed using

$$< \mathrm{r}^2(\tau) > = < MSD > = < [\mathrm{x}(\mathrm{t}+\tau) - \mathrm{x}(\mathrm{t})]^2 + [\mathrm{y}(\mathrm{t}+\tau) - \mathrm{y}(\mathrm{t})]^2 >$$

where *t* is the elapsed time and *τ* is the time lag. The complex, frequency-dependent shear modulus , *G**(*ω*), was calculated from the MSD using the generalized Stokes-Einstein relation

$$\mathrm{G}^*(\omega) = \frac{\mathrm{k}_\beta \mathrm{T}}{\pi \mathrm{i} \omega \mathrm{a} < \mathrm{r}^2(\tau) >}$$

where *a* is the bead radius and *ω* is the angular frequency, related to the time lag through *ω* = 2/ *τ*. Viscoelastic mechanical response to thermal motion was calculated from

$$|G^*(\omega)|^2 = G'(\omega)^2 + G''(\omega)^2$$

where *G*'(*ω*) and *G*''(*ω*) describe the elastic and viscous contribution, respectively. Values for *G'* were reported at a time lag of 1 second, the maximum timescale where thermal fluctuations are predominately Brownian. Video data was acquired at 54 frames per second using a high throughput microscope system described previously (41). A two-sided student *t*-test was performed on the value of the MSD at the 1-second timescale to evaluate statistical differences between cell populations.

Supplemental Figure 1.

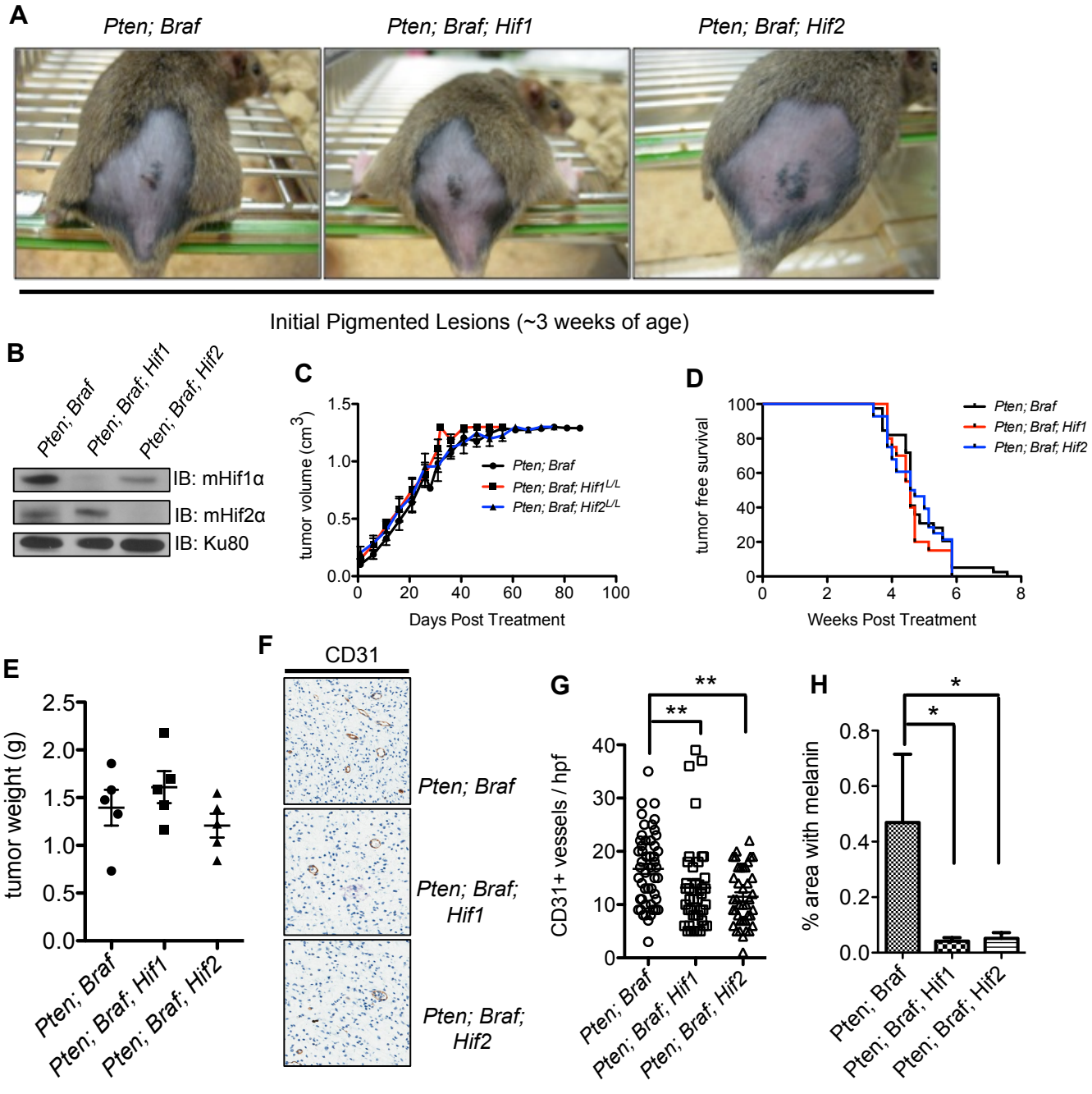

Supplemental Figure 1. Inactivation of Hif1α or Hif2α does not affect tumor free survival. (A) Representative pictures of the initial pigmented lesions on mice from the indicated genotypes seen approximately 3 weeks after tamoxifen treatment. **(B)** Tumor lysates from the indicated genotypes were immunoblotted for the indicated antibodies. **(C)** Tumor volume of primary melanomas from the indicated genotypes (*Pten; Braf,* n=39, *Pten; Braf; Hif1,* n=20, and *Pten; Braf; Hif2,* n=28). **(D)** Kaplan-Meier survival curve of cohorts of mice of the indicated genotypes (*Pten; Braf* n=39, *Pten; Braf; Hif1* n=20, and *Pten; Braf; Hif2* n=28). *P* = 0.7489, log-rank test. (**E**) Tumor weight of primary melanomas from the indicated genotype (*Pten; Braf,* n=5*, Pten; Braf; Hif1,* n=5*, Pten; Braf; Hif2,* n=5*).* **(F and G)** CD31 staining and quantification of CD31+ vessels per high power field from the indicated genotypes taken at 20X magnification (*Pten; Braf,* n=10 *Pten; Braf; Hif1,* n=8, and *Pten; Braf; Hif2,* n=8). **(H)** Quantification of the percent area of the subcapsular sinus of the lymph node expressing melanin from the indicated genotypes. Error bars = SEM ** P < 0.005, and * P < 0.05.

Supplemental Figure 2.

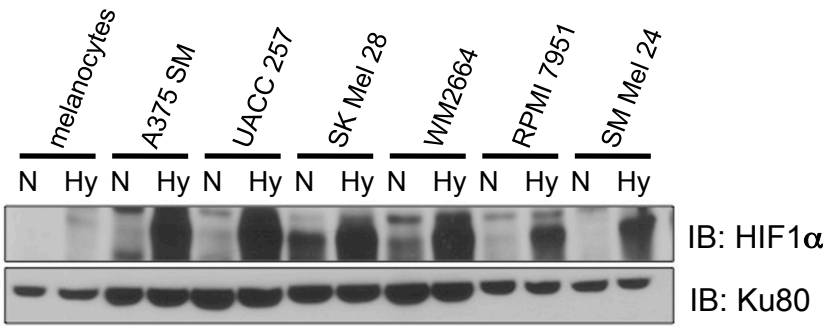

Supplemental Figure 2. A subset of melanoma cell lines express HIF1α in normoxia. The indicated cell lines were cultured overnight under normoxia or hypoxia. Whole cell extracts were prepared and immunoblotted with the indicated antibodies. This is a longer exposure of the immunoblot represented in Figure 2A.

Supplemental Figure 3.

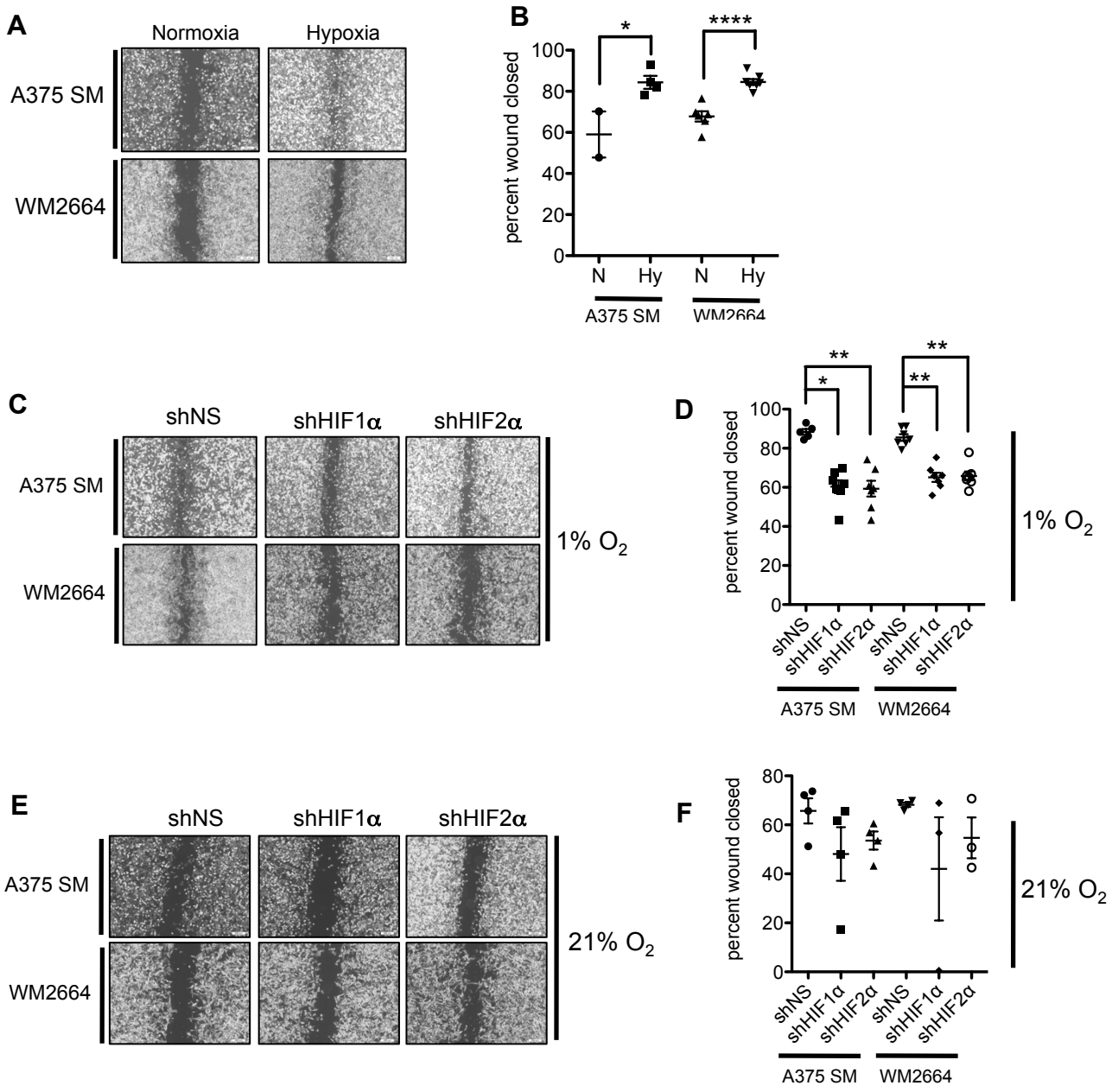

Supplemental Figure 3. Hypoxia promotes melanoma cell motility in a HIF1α and HIF2α dependent manner. (A) A375 SM and WM2664 cells were plated and allowed to reach near confluence. A scratch was generated in a uniform manner and the cells were placed in normoxia or hypoxia for 16 hours. Representative photomicrographs taken at 10X magnification demonstrate the degree of wound closure. **(B)** Quantification of wound closure from A375 SM and WM2664 cells cultured under normoxia or hypoxia. **(C)** A375 SM and WM2664 cells transfected with shRNAs against HIF1α and HIF2α were plated and allowed to reach near confluence. A scratch was generated in a uniform manner and the cells were placed in hypoxia for 16 hours. Representative photomicrographs taken at 10X magnification demonstrate the degree of wound closure. **(D)** Quantification of wound closure from A375 SM and WM2664 cells infected with shRNAs against HIF1α and HIF2α cultured under hypoxia. **(E)** A375 SM and WM2664 cells infected with shRNAs against HIF1α and HIF2α were plated and allowed to reach near confluence. A scratch was generated in a uniform manner and the cells were placed in normoxia for 16 hours. Representative photomicrographs taken at 10X magnification demonstrate the degree of wound closure. **(F)** Quantification of wound closure from A375 SM and WM2664 cells transfected with shRNAs against HIF1α and HIF2α cultured under normoxia. Error bars = SEM, *** $P < 0.0005$, ** $P < 0.005$, and * $P = 0.05$

Supplemental Figure 4.

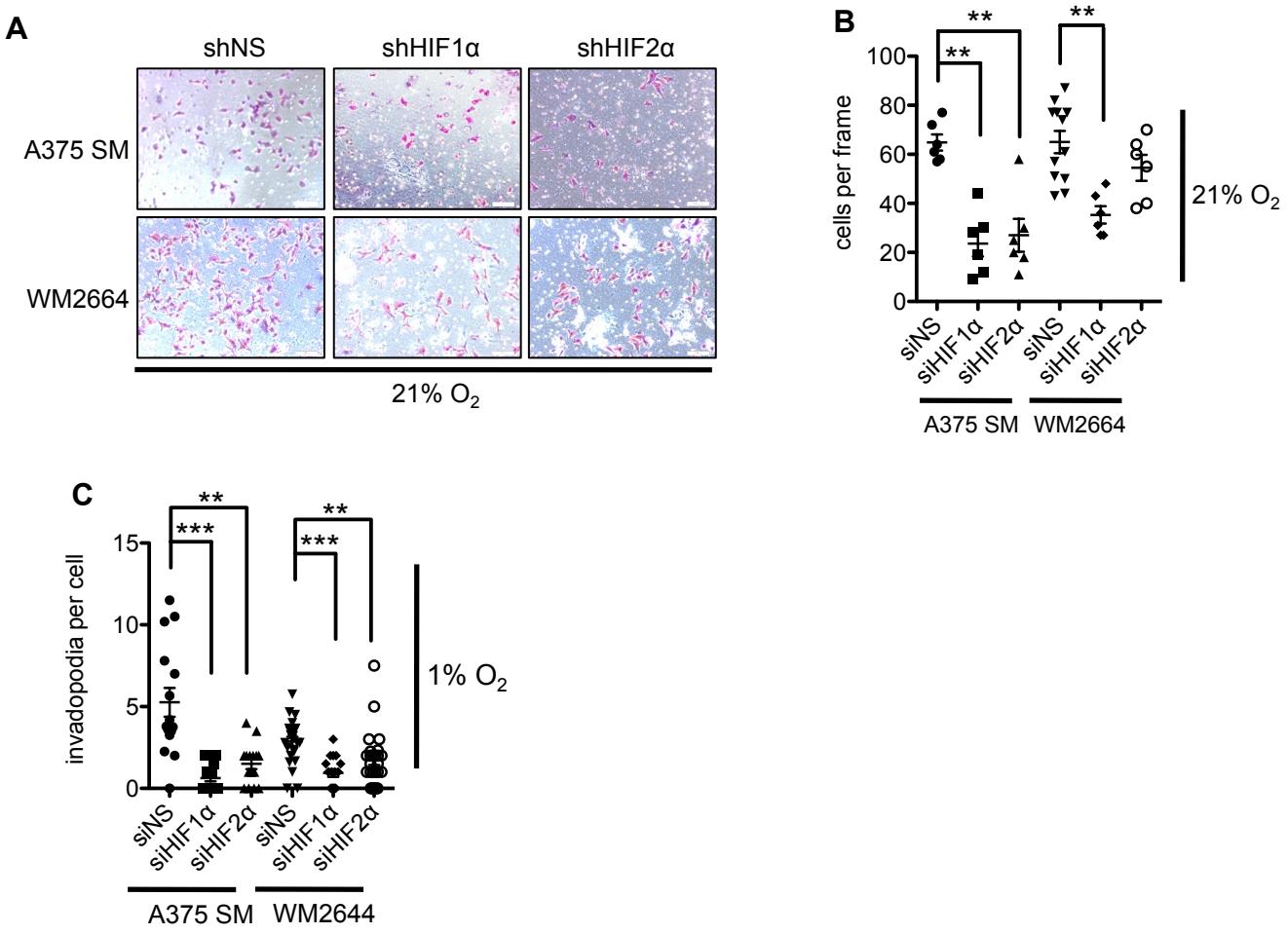

Supplemental Figure 4. Hypoxia promotes melanoma cell invasiveness in a HIF1α and HIF2α dependent manner. (A) Representative photomicrographs taken at 10X magnification of A375 SM and WM2664 cells infected with the indicated shRNAs that have invaded through matrigel chambers under normoxia. **(B)** Quantification of A375 SM and WM2664 cells infected with the indicated shRNAs that have invaded through matrigel chambers under normoxia. **(C)** Quantification of the number of invadopodia per cell in siRNA transfected A375 SM and WM2664 cells. Error bars = SEM, *** $P < 0.0005$ and ** $P < 0.005$.

Supplemental Figure 5.

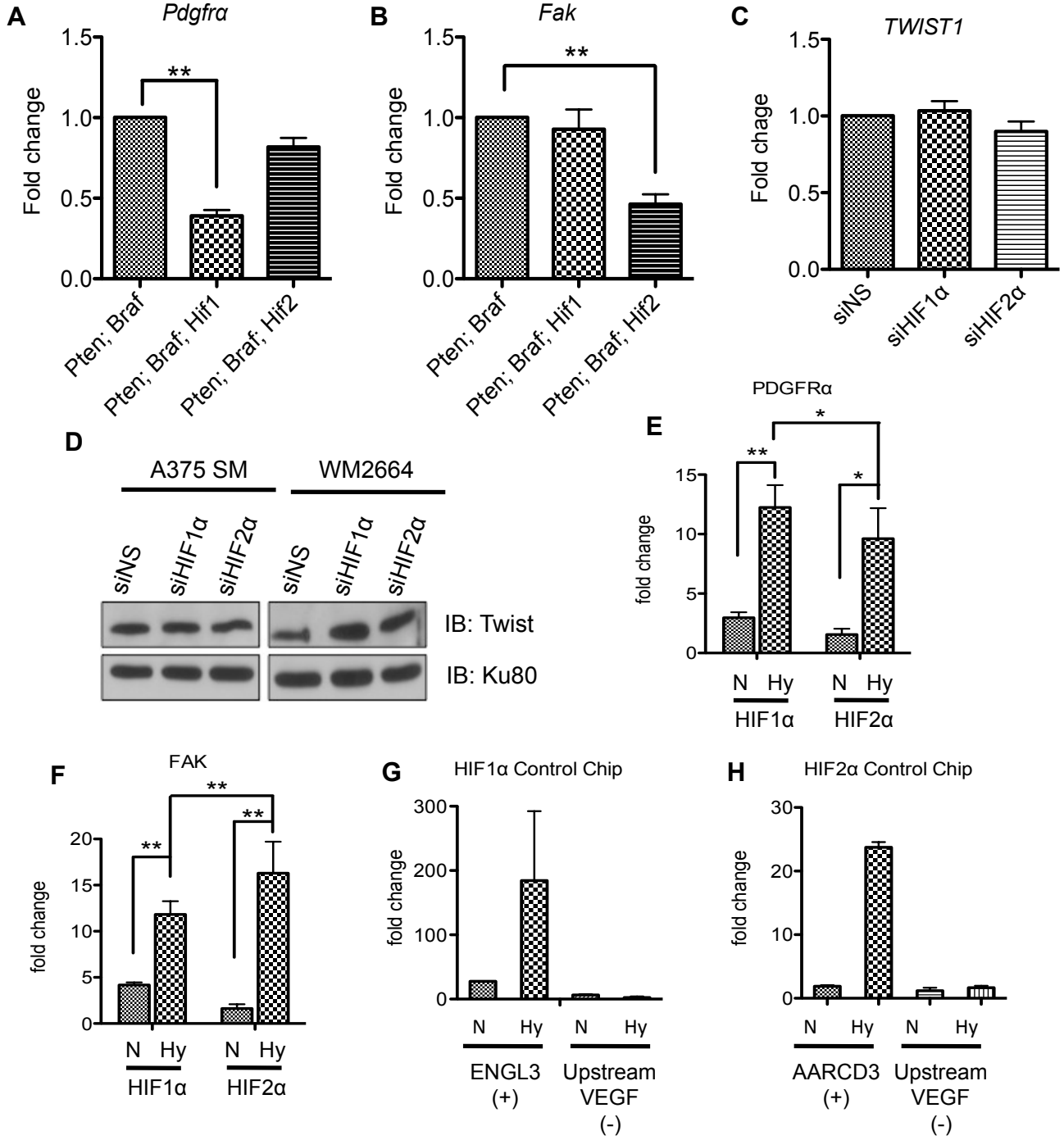

Supplemental Figure 5. HIF1α and HIF2α directly regulate PDGFRα and FAK transcription. (A and B) Total RNA was prepared from primary tumors from *Pten; Braf, Pten; Braf; Hif1$^{L/L}$, and Pten; Braf; Hif2$^{L/L}$* mice and used to perform TaqMan quantitative real time PCR for *Pdgfra* and *Fak.* **(C)** A375 SM and WM2664 cells were transfected with siRNAs against HIF1α, HIF2α, or a non-specific (NS) sequence. Total RNA was used to perform TaqMan quantitative real time PCR for *TWIST1*. **(D)** A375 SM and WM2664 cells were transfected with siRNAs against HIF1α, HIF2α, or a non-specific sequence. Whole cell lysates were immunoblotted with the indicated antibodies. **(E)** Chromatin immunoprecipitation (ChIP) of HIF1α or HIF2α at the promoter of *PDGFRA* under normoxia and hypoxia. **(F)** ChIP of HIF1α or HIF2α at the promoter of *FAK* under normoxia and hypoxia. **(G and H)** Positive (*ENGL3* and *AARCD3,* for HIF1α and HIF2α targets respectively) and negative (Upstream VEGF) controls for ChIP of HIF1α or HIF2α under normoxia and hypoxia. Error bars = SEM, ** $P < 0.005$, and * $P = 0.05$

Supplemental Figure 6

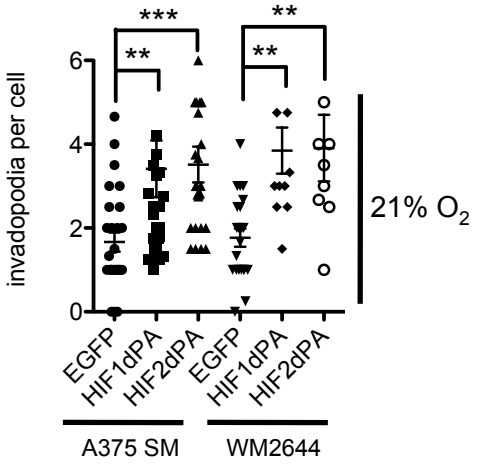

Supplemental Figure 6. HIF1α and HIF2α stabilization at normoxia increases invadopodia formation. Quantification of the number of invadopodia per cell in A375 SM and WM2664 cells stably expressing EGFP, HIF1dPA, or HIF2dPA. Error bars = SEM, *** < P 0.0005 and ** P < 0.005.

Supplemental Figure 7.

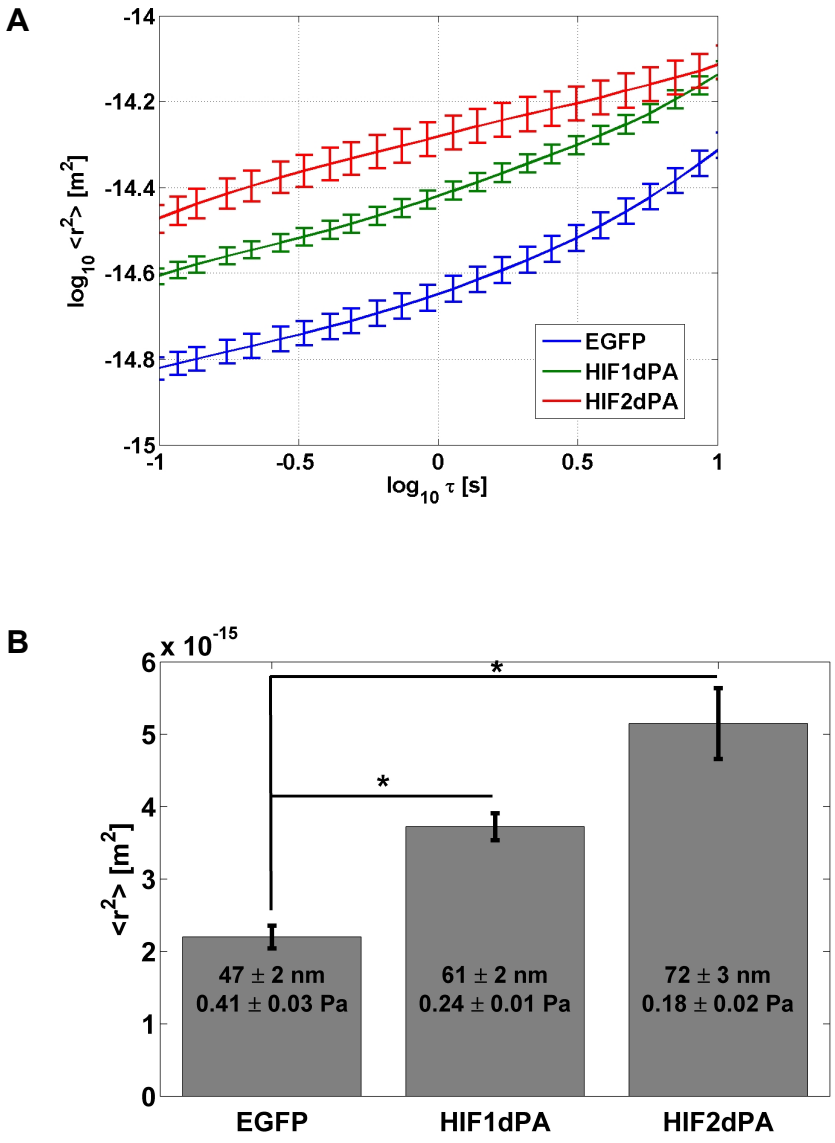

Supplemental Figure 7. Stabilized HIF1α and HIF2α decrease the stiffness of A375 SM cells. (A) Average mean squared displacement (MSD) as a function of time lag from 0.1 to 10 seconds**.** The EGFP, HIF1dPA, and HIF2dPA MSD curves are the average of 557, 519, and 190 individual particles, respectively. **(B)** Average MSD at 1-second timescale. Inside each bar is the root mean squared (RMS) displacement and the elastic shear modulus (*G*') at the 1-second time lag. The quantity for RMS displacement describes the average effective radius of the motion of a particle; the quantity for G' is an effective modulus computed using the generalized Stokes-Einstein relation (*see supplemental methods*). Error bars = SEM. * P < 0.0001.

Supplemental Figure 8.

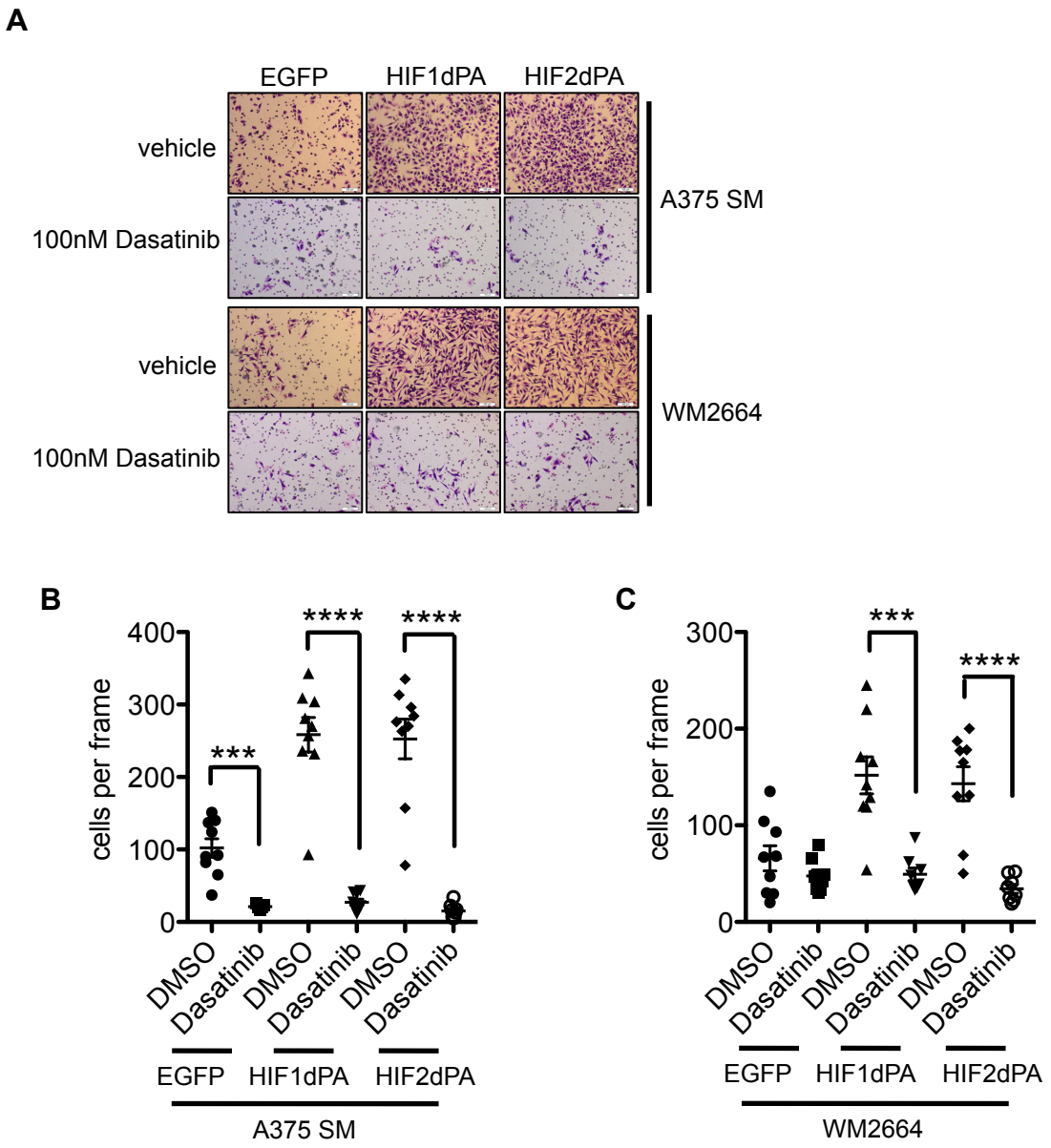

Supplemental Figure 8. Inhibition of SRC activity decreases HIF-induced invasion. (A) Representative photomicrographs taken at 10X magnification of A375 SM and WM2664 cells stably expressing EGFP, HIF1dPA, or HIF2dPA and treated with either DMSO or 100nM Dasatinib that have invaded through matrigel chambers. **(B and C)** Quantification of A375 SM and WM2664 cells stably expressing EGFP, HIF1dPA, or HIF2dPA and treated with either DMSO or 100nM Dasatinib that have invaded through matrigel chambers. Error bars = SEM, **** *P < 0.0001* and *** *P < 0.0005*

Supplemental Figure 9.

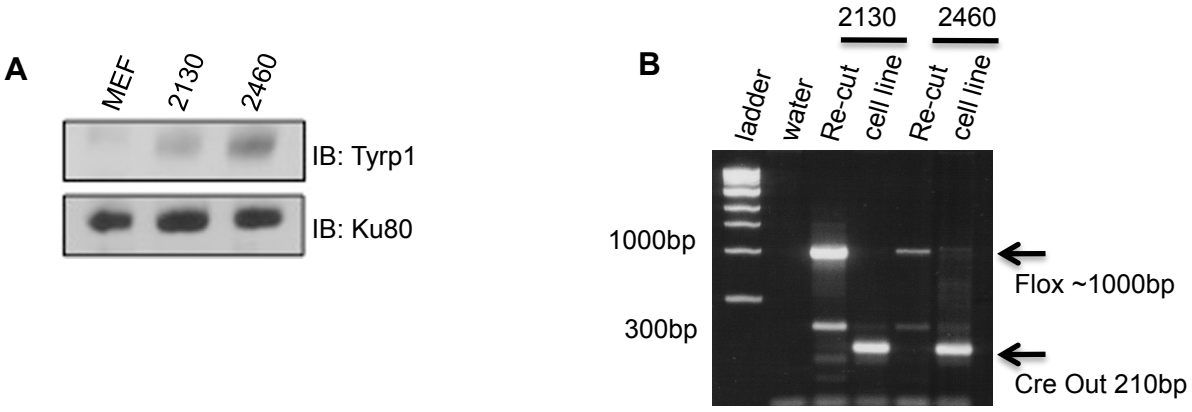

Supplemental Figure 9. Cell lines derived from primary *Pten; Braf* melanomas. (A) Whole cell extracts from cell lines derived from *Pten; Braf* melanomas (2130 and 2460) were immunoblotted with antibodies specific to Trp1. Whole cell extracts from mouse embryo fibroblasts (MEFs) were used as a negative control. **(B)** Tail DNA (recut) and cells lines of *Pten; Braf* mice (2130 and 2460) were assessed for the presence of *Pten* loss by primers that specifically detect the Floxed allele as well as the allele after Cre mediated recombination (Cre Out).

Supplemental Table 1.

construct	seed sequence
HIF1α	
shHIF1α	TGCTCTTTGTGGTTGGATCTA
HIF2α	
shHIF2α	CCATGAGGAGATTCGTGAGAA

Supplemental Table 2.

Antibody	Company	Catalogue #	Dilution
HIF1α	Cell Signaling	3716S	1:1000
HIF2α	Novus Biosystems	NB100-122	1:1000
Ku80	GeneTex	GTX70485	1:5000
pSFK	Cell Signaling	2113S	1:1000
SRC	Cell Signaling	2123S	1:1000
PDGFRα	Cell Signaling	5241S	1:500
FAK	Cell Signaling	3285S	1:1000
MT1-MMP	Millipore	AB6004	1:1000
MMP2	Cell Signaling	4022S	1:1000
MMP9	Cell Signaling	2270S	1:1000
mHif1a	Novus Biosystems	NS100-479	1:1000
mHif2a	Novus Biosystems	NB100-132	1:1000
Actin HRP	Santa Cruz	sc-1615 HRP	1:5000
Twist	Active Motif	61097	1:1000
TYRP1	Vincent Hearing		1:1000
pAKT	Cell Signaling	4060S	1:1000
AKT	Cell Signaling	9272S	1:1000
pERK	Cell Signaling	9101S	1:1000
ERK	Cell Signaling	9102S	1:1000

Supplemental Table 3.

PTEN PRIMERS	
CPF1	CTT CGG AGC ATG TCT GGC AAT GC
R1NEOCP	CTG CAC GAG ACT AGT GAG ACG TGC
PTR13	AAG GAA GAG GGT GGG GAT AC

Supplemental Table 4.

ChIP PRIMERS	
PDGFRA Forward	TAT TTA CCC CAA CCC AAG CA
PDGFRA Reverse	TGC ATG CAG TTT TCA ATG GT
FAK Forward	CCG AGA GGC TTA AGG AGG TC
FAK Reverse	GCC TCC TCG TCT TCC TCA G